Effects of cross-sectional elongation on the resistive edge modes

J. Anderson,[a] H. Nordman,[b] and J. Weiland[c]
Department of Electromagnetics, EURATOM-NFR Association, Chalmers University of Technology, Göteborg, Sweden

(Received 18 May 2000; accepted 3 October 2000)

Resistive edge modes in a shifted noncircular tokamak geometry are investigated in the electrostatic limit. The reduced Braghinskii equations are used as a model for the electrons and an advanced fluid model for the ions. An eigenvalue problem is derived from these equations which is solved numerically. It is found that the resistive ballooning modes are stabilized by plasma elongation for peaked density profiles. In addition, it is found that the resistive η_i-modes ($\eta_i = L_n/L_{T_i}$) may be either stabilized or destabilized by elongation depending on the collision frequency. © *2001 American Institute of Physics.* [DOI: 10.1063/1.1329150]

I. INTRODUCTION

The study of plasma edge turbulence and transport is a high priority issue in present day fusion research. In the edge region of a tokamak, the plasma is strongly influenced by electron–ion collisions which suggests that resistive edge modes are an important source of the turbulence. In recent years, a deeper understanding of the resistive edge modes have been attained. In particular, the role of resistive modes in the low-high ($L-H$) confinement phase transition has been thoroughly studied in Refs. 1–3 as well as the transition between linearly and nonlinearly driven turbulence in the plasma edge as given in Refs. 4 and 5.

One important effect to consider in connection with turbulence and anomalous transport is that of plasma shaping. While a considerable amount of work has been done on the effects of shaping on magnetohydrodynamic (MHD) modes, there is very little work published on the effects of shaping on drift modes. Earlier work on the η_i-mode[6–9] ($\eta_i = L_n/L_{T_i}$) stability in the core plasma have shown that elongation κ may be stabilizing or destabilizing depending on the density scale length L_n. Empirically it is found that the overall effects of elongation on the confinement time are favorable with $\tau_E \sim \kappa^{0.5}$.[10]

It is still not clear whether this favorable scaling is caused by a stabilization of the linear modes or if it is due to some indirect effects. Transport code simulations suggest that the main effects of elongation on the confinement time originates from the edge region of the plasma.[11] However, the effects of plasma shaping on the resistive edge modes are still not well known.

In the present paper, the resistive ballooning mode (RBM) and the collisional η_i-mode (i.e., η_i-modes with $\omega < \nu_{ei}$) are studied using a two fluid model. A generalized $s-\alpha$ model is used for the equilibrium which allows for variation of the parameters without recomputing the equilibrium. In particular, the effects of elongation and Shafranov shift on the stability properties of the resistive modes are investigated. It is found that for edge relevant parameters the effects of elongation are usually stabilizing, whereas the effects of Shafranov shift are rather weak.

The remainder of the paper is structured in the following way. In Sec. II the physical model and the equilibrium model is presented. In Sec. III the results and a discussion thereof is presented. Finally, in Sec. IV there is a summary.

II. FORMULATION

The reduced Braghinskii equations are used for the electron physics and an advanced fluid model is used for the ions.[12–15] This joint model is assumed to be valid in a collisional plasma which is typical in an edge plasma discharge. We have neglected electron trapping effects since the bounce frequency is assumed to be less than the electron–ion collision frequency. The effects of electromagnetic perturbations and ion sound coupling are small except in the case of very large wavelengths[1] and are hence neglected and we have neglected electron temperature perturbations for simplicity. In Ref. 1 the effects of electron temperature perturbations on the resistive edge modes are quantified. The vorticity equation, the ion continuity equation and the ion temperature equation take the forms,

$$\nabla\cdot\left(\frac{nc}{\omega_{ci}B}\frac{d}{dt}\nabla_\perp\phi\right)-\nabla\cdot(n\mathbf{v}_{\star e}+n\mathbf{v}_{\star i})-\frac{1}{e}\nabla_\parallel J_\parallel=0, \quad (1)$$

$$\frac{\partial n}{\partial t}+\nabla\cdot(n\mathbf{v}_E+n\mathbf{v}_{\star i})-\nabla\cdot\left(\frac{nc}{\omega_{ci}B}\frac{d}{dt}\nabla_\perp\phi\right)=0, \quad (2)$$

$$\frac{3}{2}n\frac{dT_i}{dt}+nT_i\nabla\cdot\mathbf{v}_i+\nabla\cdot\mathbf{q}_i=0. \quad (3)$$

Here, ϕ is the electrostatic potential, T_i is the ion temperature, $n=n_i=n_e$ is the particle density, $\mathbf{v}_i$ is the total ion drift velocity, $\mathbf{q}_i$ is the ion heat flux, $\omega_{ci}=eB/m_ic$ is the ion cyclotron frequency [$m_{i(e)}$ is the ion (electron) mass c is the speed of light and e is the electron charge], B is the magnetic field and $d/dt=(\partial/\partial t)+(\mathbf{v}_E+\mathbf{v}_{\star i})\cdot\nabla$ is the convective derivative with the diamagnetic and $\mathbf{E}\times\mathbf{B}$ velocities defined as

[a]Electronic mail: elfja@elmagn.chalmers.se
[b]Electronic mail: elfhn@elmagn.chalmers.se
[c]Electronic mail: elfjw@elmagn.chalmers.se

$$\mathbf{v}_{\star i}=\frac{c}{qnB}e_{\parallel}\times\nabla P_i, \tag{4}$$

$$\mathbf{v}_E=\frac{c}{B}e_{\parallel}\times\nabla\phi, \tag{5}$$

where q is the charge, $P_i=nT_i$ is the pressure, and $e_{\parallel}=B/|B|$ is a unit vector along the magnetic field. The ion heat flux is given by

$$\mathbf{q}_i=\mathbf{q}_{\star i}=\frac{5}{2}\frac{cT_in}{eB}e_{\parallel}\times\nabla T_i. \tag{6}$$

The parallel current, $J_{\parallel}$ is obtained from

$$J_{\parallel}=neD_{\parallel e}\left(\frac{1}{n}\nabla_{\parallel}n-\frac{e}{T_e}\nabla_{\parallel}\phi\right), \tag{7}$$

where $D_{\parallel e}=T_e/0.51m_e\nu_{ei}$ is the parallel electron diffusion and ν_{ei} is the electron–ion collision frequency. The ion temperature fluctuations couple to Eqs. (1) and (2) through

$$\nabla\cdot(n_j\mathbf{v}_{\star j})=\frac{1}{T_j}\mathbf{v}_{Dj}\cdot\nabla\delta P_j, \tag{8}$$

where δP_j $j=i,e$ is perturbed pressure and $\mathbf{v}_{Dj}$ is the magnetic drift velocity at the thermal speed, i.e.,

$$\mathbf{v}_{De}=-\rho_sc_s\left[\frac{e_{\parallel}\times\nabla B}{B}+e_{\parallel}\times\boldsymbol{\kappa}\right], \tag{9}$$

where $\boldsymbol{\kappa}=(e_{\parallel}\cdot\nabla)e_{\parallel}$. Additional curvature relations arise in Eqs. (1)–(3) as

$$\nabla\cdot\mathbf{q}_{\star}=-\tfrac{5}{2}n\mathbf{v}_{\star i}\cdot\nabla T+\tfrac{5}{2}n\mathbf{v}_{Di}\cdot\nabla T, \tag{10}$$

$$\nabla\cdot\mathbf{v}_E=\frac{q_j}{T_j}\mathbf{v}_{Dj}\cdot\nabla\phi. \tag{11}$$

Substituting the continuity equation for $\nabla\cdot\mathbf{v}$ in Eq. (3) we find that the noncurvature part of $\nabla\cdot\mathbf{q_i}$ is canceled together with the convective diamagnetic terms. The system (1)–(3) can be written as

$$\rho_s^2\left(\frac{\partial}{\partial t}-\alpha\mathbf{v}_{\star e}\cdot\nabla\right)\nabla_{\perp}^2\tilde{\phi}=-\mathbf{v}_{De}\cdot\nabla\left(\left(1+\frac{1}{\tau}\right)\tilde{n}+\frac{\tilde{t}_i}{\tau}\right)+\frac{\nabla_{\parallel}J_{\parallel}}{en}, \tag{12}$$

$$\rho_s^2\left(\frac{\partial}{\partial t}-\alpha\mathbf{v}_{\star e}\cdot\nabla\right)\nabla_{\perp}^2\tilde{\phi}=\mathbf{v}_{\star e}\cdot\nabla\tilde{\phi}+\frac{\partial\tilde{n}}{\partial t}-\mathbf{v}_{De}\cdot\nabla\left(\tilde{\phi}+\frac{\tilde{n}+\tilde{t}_i}{\tau}\right), \tag{13}$$

$$\frac{3}{2}\frac{\partial\tilde{t}_i}{\partial t}-\frac{5}{2\tau}\mathbf{v}_{De}\cdot\nabla\tilde{t}_i+\left(\frac{3}{2}\eta_i-1\right)\mathbf{v}_{\star e}\cdot\nabla\tilde{\phi}-\frac{\partial\tilde{n}}{\partial t}=0. \tag{14}$$

Here, $\tilde{n}=\delta n/n$, $\tilde{\phi}=e\phi/T_e$, and $\tilde{t}_i=\delta T_i/T_{i0}$ are the normalized perturbations of density, electrostatic potential, and ion temperature, respectively, and $\rho_s=c_s/\omega_{ci}$ with $c_s=(T_e/m_i)^{1/2}$. The dimensionless parameters are defined as $\eta_i=L_n/L_{T_i}$, $\alpha=(1+\eta_i)/\tau$, and $L_f=(d\ln f/dr)^{-1}$. The terms proportional to $\alpha\mathbf{v}_{\star e}\cdot\nabla\nabla_{\perp}^2\tilde{\phi}$ represent the finite-Larmor-radius (FLR) effects. Utilizing the standard high-n ballooning representation[16] Eqs. (12)–(14) can be written as one second-order differential equation and two algebraic equations where θ is the extended poloidal variable,

$$\frac{D_{\parallel e}}{g_{\theta\theta}q^2R^2}\frac{\partial^2(\tilde{\phi}-\tilde{n})}{\partial\theta^2}+ik_{\perp}^2\rho_s^2(\omega+\alpha\omega_{\star e})\tilde{\phi}+i\epsilon_n\omega_{\star e}g(\theta)\times\left(\tilde{n}\left(1+\frac{1}{\tau}\right)+\frac{\tilde{t}_i}{\tau}\right)=0, \tag{15}$$

$$k_{\perp}^2\rho_s^2(\omega+\alpha\omega_{\star e})\tilde{\phi}+\omega\tilde{n}-\omega_{\star e}\tilde{\phi}+\epsilon_n\omega_{\star e}g(\theta)\left(\tilde{\phi}+\frac{\tilde{n}+\tilde{t}_i}{\tau}\right)=0, \tag{16}$$

$$\left(\frac{3}{2}\omega+\frac{5}{2}\frac{\epsilon_n}{\tau}\omega_{\star e}g(\theta)\right)\tilde{t}_i-\left(\frac{3}{2}\eta_i-1\right)\omega_{\star e}\tilde{\phi}-\omega\tilde{n}=0, \tag{17}$$

where $g_{\theta\theta}$ [Eq. (24)] is a geometrical scale factor and q is the safety factor, $\omega_{\star e}=k_{\theta}\rho_sc_s/L_n$ and $\epsilon_n=\omega_D/\omega_{\star}=2L_n/L_B$. Substituting $\tilde{t}_i$ from Eq. (17) into Eqs. (15) and (16) we obtain a second-order differential eigenvalue problem in the generalized potential $\psi=\tilde{\phi}-\tilde{n}$,

$$i\frac{D_{\parallel}}{q^2R^2g_{\theta\theta}}D_1(\omega)\frac{\partial^2\psi}{\partial\theta^2}=D_2(\omega)\psi, \tag{18}$$

$$D_1(\omega)=\omega^2(1+k_{\perp}^2\rho_s^2)-\omega\omega_{\star e}\left(1-\epsilon_ng(\theta)-\frac{10}{3\tau}\epsilon_ng(\theta)-k_{\perp}^2\rho_s^2\alpha\right)+\frac{\epsilon_n}{\tau}\omega_{\star e}^2\left(\eta_i-\frac{7}{3}+\frac{5}{3}\epsilon_ng(\theta)\left[1+\frac{1}{\tau}\right]\right), \tag{19}$$

$$D_2(\omega)=k_{\perp}^2\rho_s^2(\omega+\alpha\omega_{\star e})\omega^2+\epsilon_ng(\theta)\omega\omega_{\star e}^2\times\left(1+\alpha-\epsilon_ng(\theta)\left[1+\frac{5}{3\tau}\right]\right)+\frac{(\epsilon_ng(\theta))^2}{\tau}\omega_{\star e}^3\times\left(\frac{7}{3}+\frac{5}{3\tau}-\eta_i-\frac{5}{3}\epsilon_ng(\theta)\left[1+\frac{1}{\tau}\right]\right). \tag{20}$$

Here, terms of order $\epsilon_nk_{\theta}^2\rho_s^2$ have been omitted. In the weak collisionality limit $\nu_{ei}\to0$ ($D_{\parallel}\to\infty$) a local dispersion relation $D_1(\omega,\theta=0)=0$ (Ref. 12) may be obtained, which describes the toroidal η_i-mode. Moreover, in the large collisionality limit $\nu_{ei}\to\infty$ ($D_{\parallel}\to0$) the resistive ballooning mode dispersion relation is obtained and for $D_{\parallel}=0$ it simplifies to the ideal interchange mode equation $[D_2(\omega,\theta=0)=0]$ that contains effects of finite ϵ_n and η_i. Thus the eigenmode equation (18) contains two branches, an electron branch driven by collisions and curvature and an ion branch driven by curvature and ion temperature gradients.

In the second-order differential equation the geometry dependent factors are the magnetic drift frequency ω_D and the scale factor $\sqrt{g_{\theta\theta}}$ and in addition the geometry also modi-

fies $k_\perp^2$. As a model for the equilibrium, we employ the generalized $s-\alpha$ equilibrium model of Ref. 17, which allows for modification of equilibrium parameters like elongation and Shafranov shift without recomputing the equilibrium. The flux coordinate system is defined by

$$R(r,\theta)=\sum_{n=0}^{\infty} R_n(r)\cos(n\theta), \tag{21}$$

$$Z(r,\theta)=\sum_{n=0}^{\infty} Z_n(r)\sin(n\theta), \tag{22}$$

where R and Z are the usual cylindrical coordinates. The terms R_0, $R_1=r$, $Z_1=r\kappa$ describes shift, minor radius and ellipticity, respectively, the terms R_2, Z_2 describes triangularity. In the present work effects of triangularity are neglected. The scale factors become

$$g_{rr}=(\partial_r R_0+\cos\theta)^2+(\partial_r(r\kappa)\sin\theta)^2, \tag{23}$$

$$g_{\theta\theta}=r^2(1+(\kappa^2-1)\cos^2\theta), \tag{24}$$

$$g_{r\theta}=\partial_r(\kappa r)\kappa r\sin\theta\cos\theta-r(\partial_r R_0+\cos\theta)\sin\theta, \tag{25}$$

$$g_{\phi\phi}=R^2, \tag{26}$$

where κ is the elongation and $\partial_j=\partial/\partial x^j$, note that it only acts at the object directly after and we denote position vector $\mathbf{r}=(R,Z)$ and basis vectors $\hat{e}_j=(1/h_j)\partial_j\mathbf{r}$. The metric tensor g_{ij} is defined as

$$ds^2=g_{ij}dx^i dx^j. \tag{27}$$

Keeping only the first terms in ϵ-ordering and with the B-field given by $\mathbf{B}=B_\theta\hat{\theta}+B_\phi\hat{\phi}$, we have the magnetic drift frequency and $k_\perp$ as

$$\frac{\omega_D}{\omega_{\star e}}=\epsilon_n g(\theta)\approx\frac{\epsilon_n}{\sqrt{g_{\phi\phi}}}\left(g^{\theta r}\Gamma^r_{\phi\phi}J\frac{q}{r}s\theta+g^{\theta\theta}\Gamma^r_{\phi\phi}Jq-g^{rr}\Gamma^\theta_{\phi\phi}J\frac{q}{r}s\theta-g^{\theta r}\Gamma^\theta_{\phi\phi}Jq\right), \tag{28}$$

$$k_\perp^2=k_\theta^2 k(\theta)\approx+\frac{k_\theta^2}{J^2}(g_{rr}+g_{\theta\theta}(s\theta)^2-2g_{r\theta}s\theta), \tag{29}$$

where $s=d\ln q/d\ln r$ is the global magnetic shear. Here the inverse of the metric tensor is defined by the relation $g_{ij}g^{jk}=\delta_i^k$ compare with Eq. (33). The Christoffel symbols are given by

$$\Gamma^j_{ik}=\tfrac{1}{2}g^{jn}(\partial_k g_{ni}+\partial_i g_{nk}-\partial_j g_{ik}), \tag{30}$$

$$\Gamma^r_{\phi\phi}=-\frac{1}{4}\left(\frac{g_{\theta\theta}}{J^2}\partial_r g^2_{\phi\phi}-\frac{g_{r\theta}}{J^2}\partial_\theta g^2_{\phi\phi}\right), \tag{31}$$

$$\Gamma^\theta_{\phi\phi}=-\frac{1}{4}\left(-\frac{g_{\theta r}}{J^2}\partial_r g^2_{\phi\phi}+\frac{g_{rr}}{J^2}\partial_\theta g^2_{\phi\phi}\right), \tag{32}$$

where the Jacobian is given by

$$J^2=g_{\phi\phi}(g_{rr}g_{\theta\theta}-g^2_{r\theta}). \tag{33}$$

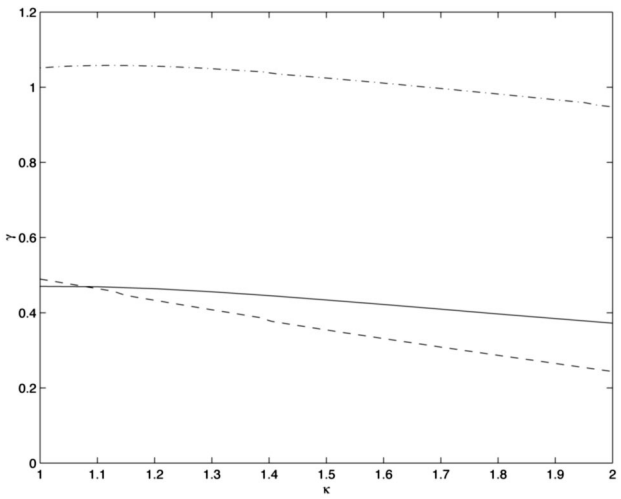

FIG. 1. The growth rate (normalized to the electron diamagnetic drift frequency) vs κ, for $q=s=\tau=1$, $k_\perp^2\rho^2=0.1$, $\eta_i=3$, $\nu_{ei}=0.05$, $\epsilon_n=1$ (dashed–dotted line); $\epsilon_n=0.1$ (dashed line); $\epsilon_n=0.1$ (solid line) the noncollisional advanced fluid model.

These results reduce to the usual expressions in circular geometry, i.e.,

$$\frac{\omega_D}{\omega_{\star e}}\approx\epsilon_n(\cos\theta+s\theta\sin\theta), \tag{34}$$

$$k_\perp^2\approx k_\theta^2(1+s^2\theta^2). \tag{35}$$

III. RESULTS AND DISCUSSION

The solutions to the eigenmode equation [Eq. (18)] are found by a numerical standard shooting technique. We assume that the even modes are more important than the odd modes for the curvature driven modes studied here. Applying the shooting technique we start from $\theta=0$ with $\psi(0)=1$ and $\psi'(0)=0$, and iterate the eigenvalues until the condition $\psi\to 0$ as $\theta\to\infty$ is satisfied. In the following analysis it is important to note that the growth rates of the resistive ballooning modes (RBM) and the η_i-modes are of the same order but the maximum growth rate occurs at different length scales, $k_\theta\rho\approx 0.15$ for the RBM and $k_\theta\rho\approx 0.3$ for the η_i-modes. We divide the results and discussion section in two parts starting with the collisional η_i-modes and then followed by a discussion of the RBM. Henceforth the collision frequency will be normalized as in Ref. 18 with $\nu_{ei}^\star=q^2R/\lambda_e(m_e/m_i)^{1/2}$ and $\lambda_e=v_{the}/\nu_{ei}$.

In Fig. 1 the effects of elongation κ on the η_i-mode is displayed. The growth rate (normalized to the diamagnetic frequency) as a function of elongation with ϵ_n $(2L_n/L_B)$ as a parameter is shown. The other parameters are $q=s=\tau=1$, $k_\perp^2\rho^2=0.1$, $\eta_i=3$, and $\nu_{ei}=0.05$. The results are illustrated for $\epsilon_n=1.0$ (dashed–dotted line) and $\epsilon_n=0.1$ (dashed line). As observed, a weak stabilization with elongation is obtained. In the flat density case ($\epsilon_n=1.0$) the corresponding analytical limit eigenvalue from the collisionless advanced fluid model gives $\gamma/\omega_\star=1.01$ at $\kappa=1$, which is in rather good agreement with the numerical result. The collisional η_i-mode growth (dashed line) is similar to that obtained

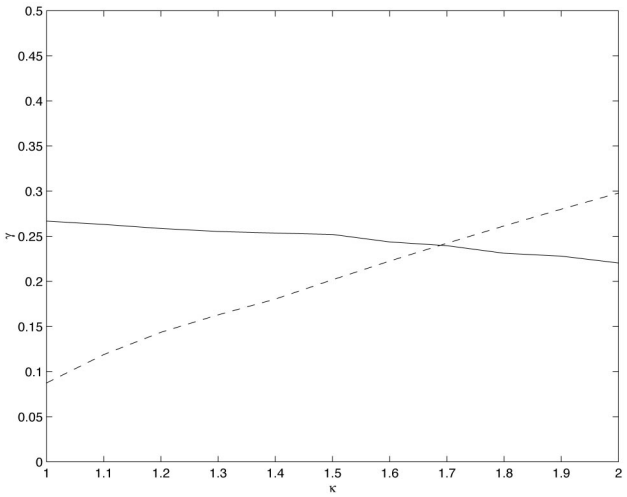

FIG. 2. The growth rate (normalized to c_s/L_n) vs κ, for $q=2$, $s=\tau=1$, $k_\perp^2\rho^2=0.16$, $\epsilon_n=0.33\eta_i=6$, $\nu_{ei}=0.01$ (solid line) and $\nu_{ei}=0.25$ (dashed line).

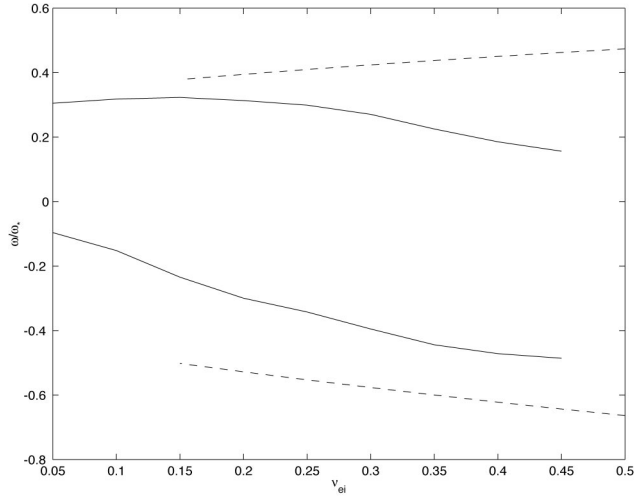

FIG. 3. The eigenfrequency (normalized to the electron diamagnetic drift frequency) vs ν_{ei} for $q=s=\tau=1$, $k_\perp^2\rho^2=0.1$, $\eta_i=2$, $\epsilon_n=0.1$ (solid line) and $\epsilon_n=0.15$ (dashed line).

(solid line) by a collisionless advanced fluid model including parallel ion motion[12,9] for peaked density profiles $\epsilon_n=1$. This collisionless model is based on an advanced fluid model for the ions whereas the electrons are assumed to be Boltzmann distributed. When the effect of parallel ion motion is small ($\omega \gg k_\parallel c_s$) the two models give similar results since the collisional effects on the η_i-mode are rather weak.

Next, in Fig. 2 the growth rate (normalized to c_s/L_n) as a function of elongation with ν_{ei} as a parameter is given. The other parameters are taken from Ref. 8 with $q=2$, $s=\tau=1$, $k_\perp^2\rho^2=0.16$, $\eta_i=6$, and $\epsilon_n=0.33$. For medium collisionality $\nu_{ei}=0.25$ (dashed line) a destabilization with increasing elongation is found whereas for low collisionality $\nu_{ei}=0.01$ (solid line) the favorable elongation scaling is recovered, the latter case has been observed in recent work, by both gyrokinetic[8] and collisionless fluid[9] simulations.

However, a more detailed study shows a slightly more colorful picture. Expanding around the collisionless solution ω_0 to the local dispersion relation with $\omega=\omega_0+\delta\omega$ and then solving for $\delta\omega$, gives us

$$\delta\omega=\frac{c\nu_{ei}D_2(\omega_0)}{\dfrac{\partial D_1(\omega_0)}{\partial\omega}}. \tag{36}$$

Thus the imaginary part of $\delta\omega$ is

$$\mathrm{Im}(\delta\omega)\approx C\frac{\nu_{ei}}{\gamma}(-k_\perp^2\rho^2\omega_r^3-k_\perp^2\rho^2\alpha\omega_\star\omega_r^2 - \epsilon_n g(1+\alpha)\omega_\star^2\omega_r). \tag{37}$$

Here $\omega_0=\omega_r+i\gamma$ and $\omega_r=1-\epsilon_n g-(10/3\tau)\epsilon_n g-\alpha k_\perp^2\rho^2$ and we have assumed that $\gamma \ll \omega_r$. Equation (37) is not positive definite and may have both positive or negative sign, indicating that collisions may have either stabilizing or destabilizing effects on the η_i-mode.

In Fig. 3 the eigenfrequency (both real frequency and growth rate normalized to the diamagnetic frequency) as a function of collision frequency is displayed. The parameters are as in Fig. 1, except that $\eta_i=2$, $\kappa=1$, $\epsilon_n=0.1$ (solid lines), and $\epsilon_n=0.15$ (dashed lines). For $\epsilon_n=0.15$ a destabilization with increasing collision frequency is found, whereas for $\epsilon_n=0.1$ a stabilization is found. The η_i-mode growth rate scales rather weakly with collision frequency.

Now the RBM is to be considered. In earlier work[19] it was shown that the spectrum of the instability is very broad. Shown in Fig. 4, the other parameters are $s=q=\tau=1$, $\epsilon_n=0.1$, $\nu_{ei}=0.33$, $\eta_i=0$ is the growth rate (normalized to the diamagnetic frequency) as a function of the magnetic shear s with mode number $m=k_\theta\rho_s(\nu_{ei}/\epsilon_n)^{1/2}$ as a parameter (the other parameters are $s=q=\tau=1$, $\epsilon_n=0.1$, $\nu_{ei}=0.33$, $\eta_i=0$). It is found that for high $m=1.77$ (solid line) and medium $m=0.88$ (dashed line) the growth rate initially increases and then above $s=1$ it rapidly decreases but for low $m=0.35$ (dashed–dotted line) the growth rate increases with

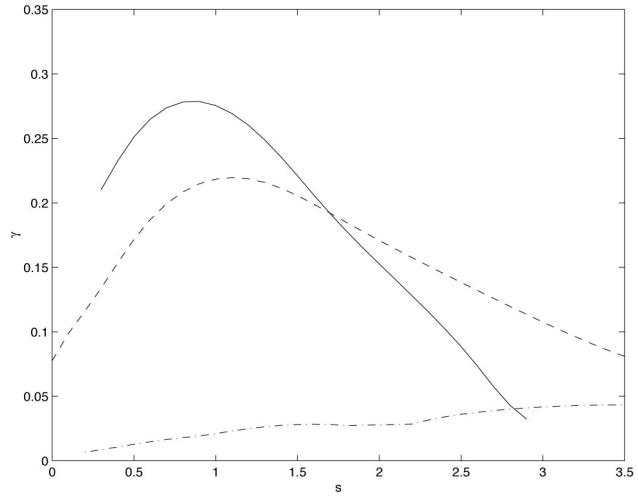

FIG. 4. The growth rate (normalized to the diamagnetic frequency) vs s. For $q=s=\tau=1$, $\eta_i=0$, $\epsilon_n=0.1$, $\nu_{ei}=0.33$ with $m=1.77$ (solid line), $m=0.88$ (dashed line), and $m=0.35$ (dashed–dotted line).

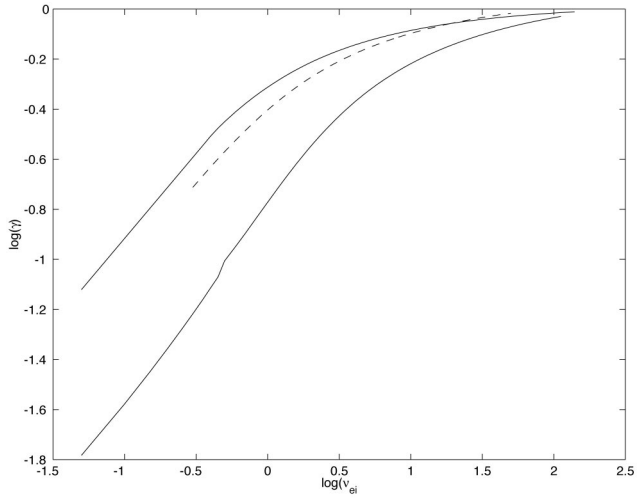

FIG. 5. The growth rate (normalized to the electron diamagnetic drift frequency) vs ν_{ei} for $s=q=\tau=1$, $\epsilon_n=0.1$ with $k_\perp\rho=0.075$ (solid line), $k_\perp\rho=0.15$ (dashed line), and $k_\perp\rho=0.3$ (dotted line).

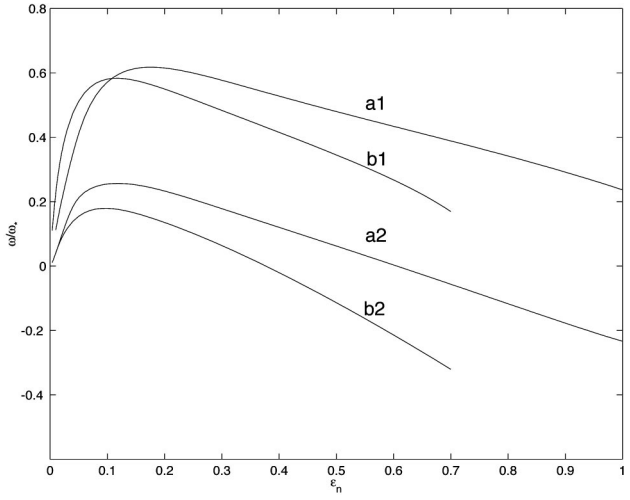

FIG. 6. The growth rate (normalized to the electron diamagnetic drift frequency) vs ϵ_n for $q=s=\tau=1$, $k_\perp\rho=0.15$, $\eta_i=0$; b1 and b2 ($\kappa=1$); a1 and a2 ($\kappa=1.5$).

increasing magnetic shear. This is in good quantitative agreement with the results found in Ref. 19.

Next, we investigate the growth rate [normalized to $\gamma_0=(2c_s^2/RL_n)^{1/2}$] as a function of the collision frequency with FLR as a parameter. This is shown in Fig. 5 in a log–log plot with parameters as in Fig. 4 with $k_\theta\rho=0.075$ (solid line), $k_\theta\rho=0.15$ (dashed line), and $k_\theta\rho=0.3$ (dotted line). From these three graphs we obtain the ν_{ei} dependence of the mode as $\gamma\sim\nu_{ei}^{0.8}$ (solid line, small values of the FLR parameter) and $\gamma\sim\nu_{ei}^{1.0}$ (dashed–dotted line, $k_\theta\rho=0.15$). The results reflects the presence of two different branches of the resistive modes that differ in the scaling with ν_{ei} as $\gamma\sim\nu_{ei}^{0.33}$ (resistive ballooning mode) and $\gamma\sim\nu_{ei}^{1.0}$ (resistive drift waves), respectively.[3] The former estimate may be unattainable in this case since the average curvature may not be small compared to the FLR as assumed in the analytical estimate. For large collisionality, the growth rates approach the ideal MHD limit γ_0 as expected from Eq. (18).

In Fig. 6 we illustrate the ϵ_n dependence of the eigenvalue (both real frequency and growth rate normalized to the diamagnetic frequency) with κ as a parameter. The other parameters are $s=q=\tau=1$, $\eta_i=0$, $k_\theta\rho=0.15$, $\nu_{ei}=0.5$ with $\kappa=1$ (curves b1, b2) and $\kappa=1.5$ (curves a1, a2). The effects of elongation is stabilizing for peaked density profiles ($\epsilon_n\leqslant 0.1$) typical for an edge plasma discharge whereas in the flat density limit the effects are destabilizing. However, for large ϵ_n the mode is stabilized due to compressional effects. The results found here are very similar to the results found for the η_i-mode in the collisionless advanced fluid model (cf. Fig. 2 in Ref. 9).

In order to clarify the effects of elongation on the RBM, an investigation of the isolated effects of ω_D, $k_\perp$, $k_\parallel$ is performed. In Fig. 7 the growth rate (normalized to the diamagnetic frequency) as a function of elongation is displayed. The other parameters are as in Fig. 6. Figure 7 shows the growth rate in three different cases; all elongation effects included (solid line), without elongation effects on ω_D (dashed line), and both ω_D and $k_\perp$ kept at their circular value (dashed–dotted line). It is observed that ω_D contributes with a substantial stabilization and $k_\perp$, $k_\parallel$ contribute with a destabilizing effect. This is in agreement with the results obtained for the η_i-mode in the collisionless fluid model (cf. Fig. 7 in Ref. 9), where it was found that the stabilizing effects were due to elongation effects on ω_D while the elongation effects on $k_\perp$ were destabilizing for the relevant parameters.

The effects of elongation on the k_θ-spectrum are studied, in Fig. 8. The mode growth (normalized to the diamagnetic frequency) as a function of $k_\theta^2\rho^2$ with κ as a parameter is shown. The other parameters are $s=q=\tau=1$, $\epsilon_n=0.2$, $\eta_i=0$, $\nu_{ei}=0.15$, and $\kappa=1$ (solid line) and $\kappa=1.5$ (dashed line). One important feature of this mode is that the maximum growth occurs at $k_\theta\rho=0.15$, for both $\kappa=1$ and $\kappa=1.5$. A small destabilization is found around $k_\theta\rho\approx 0.15$ for $\kappa=1.5$, but for larger values of κ a stabilization with elon-

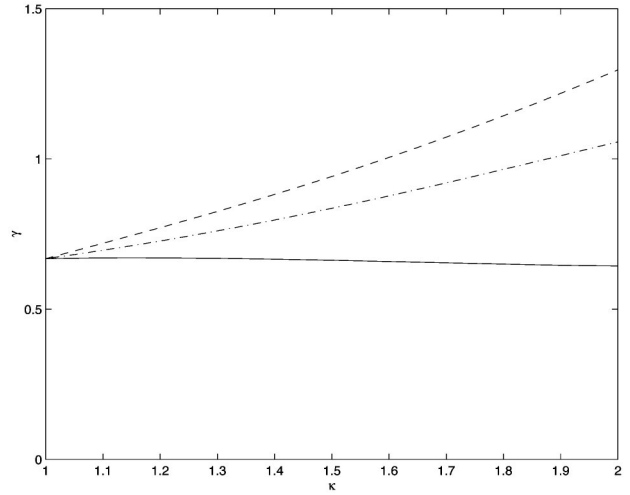

FIG. 7. The growth rate (normalized to the electron diamagnetic drift frequency) vs elongation for $q=s=\tau=1$, $k_\perp\rho=0.15$, $\epsilon_n=0.1$, $\eta_i=0$ with (solid line) as the full numerical simulations and (dashed line) as the simulation with $\omega_D(\theta,\kappa=1)$ and the (dashed–dotted line) is with both ω_D and $k_\perp$ at their circular value.

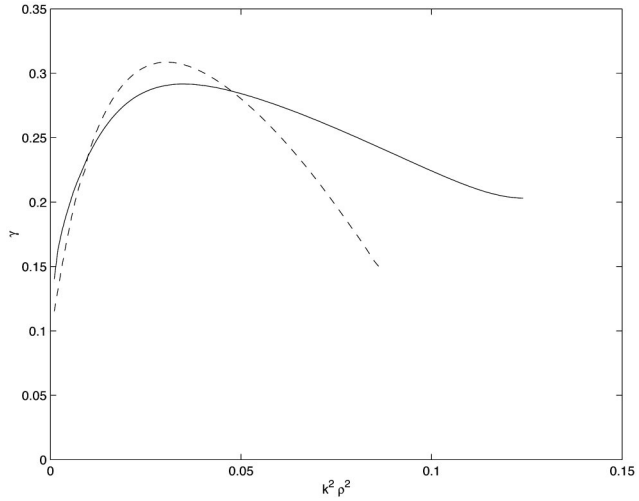

FIG. 8. The growth rate (normalized to the electron diamagnetic frequency) vs $k^2\rho^2$ with $q=s=\tau=1$, $\epsilon_n=0.2$, $\eta_i=0$ where $\kappa=1$ (solid line) and $\kappa=1.5$ (dashed line).

gation may be recovered. It is also noted that for shorter wavelengths the mode growth decreases more rapidly for $\kappa=1.5$ than $\kappa=1$.

In a recent analytical paper[18] it was found that the resistive ballooning mode is stabilized by an increase in η_i, already for small values of η_i. In Fig. 9 the eigenfrequency (normalized to the diamagnetic frequency) as a function of η_i is displayed with parameters from Ref. 18 as $s=2$, $q=\tau=1$, $\epsilon_n=0.08$, $k_\theta\rho=0.15$, and $\nu_{ei}=0.25$. The stabilization of the growth rate with an increase in η_i is preserved and it is found that it is even enhanced by an additional elongation stabilization. However, as η_i increases an η_i driven mode starts to grow and may overshadow the favorable stability properties of the RBM, this occurs for $\eta_i \geqslant 1$.

The effects of the Shafranov shift were also investigated and it was found to contribute with only modest modifications of the results presented here.

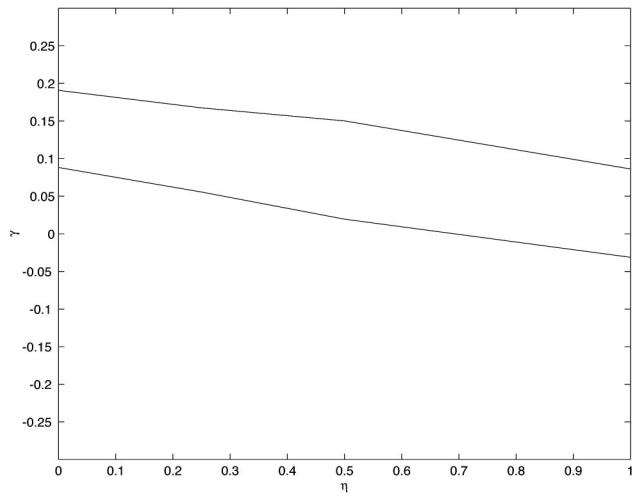

FIG. 9. The eigenfrequency (normalized to the electron diamagnetic drift frequency) vs η_i for $q=\tau=1$, $s=2$, $k_\perp\rho=0.15$, $\epsilon_n=0.08$.

IV. SUMMARY

In the plasma edge region, the two linear instabilities expected to dominate in the electrostatic limit are the resistive ballooning mode and the η_i-mode. The effects of plasma elongation and Shafranov shift on these instabilities are investigated using the analytical noncircular equilibrium model of Ref. 17. The work is based on the Braghinskii equations as a model for the electrons together with an advanced fluid model for the ions. The resistive edge modes are investigated in a noncircular equilibrium. An eigenvalue equation [Eq. (18)] is derived and solved numerically using a shooting technique. The geometrical effects enter Eq. (18) through the magnetic drift frequency ω_D and through the perpendicular ($k_\perp$) and the parallel ($k_\parallel$) length scales. It is found that the effects of elongation on the resistive η_i-mode are usually weakly stabilizing for edge relevant parameters, in agreement previous results obtained for reactive η_i-modes.[9] In addition, it is found that the effects of collisions on the resistive η_i-modes are rather weak and may be either stabilizing or destabilizing. For the resistive ballooning mode, stabilization due to elongation is found for edge like parameters, whereas for large $\epsilon_n=2L_n/L_B$, a destabilization is obtained. In particular, the η_i stabilization of the strongest mode observed in Ref. 18 is further enhanced if the effects of elongation are taken into account, as exemplified by Fig. 9. In conclusion, the elongation scaling of the η_i- and ballooning modes seem to be more favorable in the edge, where ϵ_n is small, than in the core. As suggested by recent transport code simulations, the scaling originating from the edge may be more important for determining the total effects of plasma elongation on the energy confinement.[11] However, to draw conclusions of the effects of elongation on the confinement time a more extensive study using a transport code which treats both the edge and core transport processes self-consistently is needed.

[1] D. R. McCarthy, P. N. Guzdar, and J. F. Drake, Phys. Fluids B **4**, 1846 (1992).
[2] P. N. Guzdar, J. F. Drake, D. R. McCarthy *et al.*, Phys. Plasmas **5**, 3712 (1993).
[3] B. D. Scott, Plasma Phys. Controlled Fusion **39**, 1635 (1997).
[4] B. D. Scott, Phys. Rev. Lett. **65**, 3284 (1990).
[5] A. Zeiler, D. Biskamp, J. F. Drake *et al.*, Phys. Plasmas **7**, 2654 (1998).
[6] D. D. Hua, Y. Q. Yu, and T. K. Fowler, Phys. Fluids **34**, 3216 (1992).
[7] J. Kesner, Nucl. Fusion **31**, 511 (1991).
[8] R. E. Waltz and R. L. Miller, Phys. Plasmas **6**, 4265 (1999).
[9] J. Anderson, H. Nordman, and J. Weiland, Plasma Phys. Controlled Fusion **42**, 545 (2001).
[10] P. N. Yshmanov *et al.*, Nucl. Fusion **30**, 1999 (1990).
[11] G. Bateman (private communications, 2000).
[12] A. Jarmèn, P. Andersson, and J. Weiland, Nucl. Fusion **27**, 941 (1987).
[13] J. Nilsson, M. Liljeström, and J. Weiland, Phys. Fluids B **2**, 2568 (1990).
[14] S. C. Guo and J. Weiland, Nucl. Fusion **37**, 1095 (1997).
[15] J. Weiland, *Collective Modes in Inhomogeneous Plasmas, Kinetic, and Advanced Fluid Theory* (IOP Publishing, Bristol, 2000), p. 114.
[16] J. W. Connor, R. J. Hastie, and J. B. Taylor, Proc. R. Soc. London, Ser. A **365**, 1 (1979).
[17] R. L. Miller, M. S. Chu, J. M. Greene *et al.*, Phys. Plasmas **5**, 973 (1998).
[18] R. Singh, H. Nordman, J. Anderson *et al.*, Phys. Plasmas **5**, 3669 (1998).
[19] S. V. Novakovskii, P. N. Guzdar, J. F. Drake *et al.*, Phys. Plasmas **2**, 781 (1995).